

AN EXPERIMENTAL INVESTIGATION OF MULTISOLITON GENERATION USING AN ERBIUM-DOPED FIBER AMPLIFIER AND A FIBER OPTIC RING RESONATOR

J. Ali¹ and P. P. Yupapin²

¹Institute of Advanced Photonics Sciences, Science Faculty, Universiti Teknologi Malaysia, 81310 Skudai, Johor Bahru, Malaysia

²Advanced Research Center for Photonics, Faculty of Science, King Mongkut's Institute of Technology Ladkrabang, Bangkok 10520, Thailand; Corresponding author: kypreech@kmitl.ac.th

Received 24 April 2009

ABSTRACT: We have successfully generated the mutisoliton pulses using a Gaussian pulse in a fiber optic ring resonator incorporating an erbium-doped fiber (EDF) and a semiconductor optical amplifiers (SOAs). The multisoliton memory time within the system is also measured. Initially, the Gaussian input pulse is pumped and amplified through the EDF and the SOAs, respectively. The suitable experimental values, such as drive current, coupling power, and the fiber ring radius, are arranged to generate the multisoliton pulses. In application, the wider multisoliton band can be generated by adjusting the suitable system parameters. Results obtained have shown that the multisoliton with a free spectrum range and spectrum width of 2.4 and 0.96 nm is achieved. The memory time and the maximum soliton output of 15 min and of 5.94 dBm, respectively, are noted. © 2009 Wiley Periodicals, Inc. *Microwave Opt Technol Lett* 52: 70–72, 2010; Published online in Wiley InterScience (www.interscience.wiley.com). DOI 10.1002/mop.24834

Key words: multisoliton; Gaussian soliton; fiber optic ring resonator; erbium fiber amplifier

1. INTRODUCTION

Multisoliton light source generation becomes the interesting research technique that can be used to drastically increase the communication channel capacity, while the high optical output is the second advantage for long distance link. In principle, there are two techniques that can be used to generate the soliton pulses. First, Pornsuwancharoen et al. [1] have shown that the soliton pulses can be generated theoretically using a pumped soliton pulse within a microring resonator system; moreover, the large signal amplification is also achieved. Second, a Gaussian soliton can be generated, whereas the simple system arrangement can be setup to form the soliton pulse within the medium. This technique becomes a more attractive tool in the area for soliton generation and investigation. Generally, the basic requirement of the pumped soliton and Gaussian soliton is the intense input light into the system, where there are two ways to reach the requirement: (i) using high-power light source and (ii) reduce the media length, that is, ring radius. However, there are many research works have reported in both theoretical and experimental works using a common Gaussian pulse for soliton study [2]. For further reading, many earlier works of soliton applications in either theory or experimental works are found in a soliton application book by Hasegawa [3]. Many of the soliton-related concepts in fiber optic are discussed by Agrawal [4]. However, the problems of soliton–soliton interactions [5], collision [6], rectification [7], and dispersion management [8] are required to solve and address. Therefore, in this work, a common laser source (Gaussian pulse) is used, whereas the use of a Gaussian pulse to form a multisoliton using a fiber ring resonator is recommended [9]. In practice, the intense pulse is obtained by using the erbium-doped fiber (EDF) and semiconductor amplifiers incorporating in the experimental setup.

The multisoliton band is formed by the modulated signals through the connecting fiber ring resonator. The other problems such as low output power and soliton collision can be solved using the free spectrum range design [10].

2. EXPERIMENT

Light from a monochromatic light source is launched into a ring resonator with constant light field amplitude (E_0) and random phase modulation (ϕ_0), which results in temporal coherence degradation. Hence, the time-dependent input light field (E_{in}), without pumping temperature, can be expressed as

$$E_{in}(t) = E_0 \exp^{j\phi_0(t)} \quad (1)$$

We assume that the nonlinearity of the optical fiber ring is of the Kerr-type, that is, the refractive index is given by

$$n = n_0 + n_2 I = n_0 + \left(\frac{n_2}{A_{eff}} \right) P, \quad (2)$$

where n_0 and n_2 are the linear and nonlinear refractive indexes, respectively. I and P are the optical intensity and optical power, respectively. The effective mode core area of the device is given by A_{eff} .

When a Gaussian pulse is input and propagated within a fiber ring resonator, the resonant output is formed; thus, the normalized output of the light field is the ratio between the output and input fields ($E_{out}(t)$ and $E_{in}(t)$) in each roundtrip, which can be expressed as [9]

$$\left| \frac{E_{out}(t)}{E_{in}(t)} \right|^2 = (1 - \gamma) \times \left[1 - \frac{(1 - (1 - \gamma)x^2)\kappa}{(1 - x\sqrt{1 - \gamma}\sqrt{1 - \kappa})^2 + 4x\sqrt{1 - \gamma}\sqrt{1 - \kappa}\sin^2\left(\frac{\phi}{2}\right)} \right]. \quad (3)$$

Equation (3) indicates that a ring resonator in the particular case is similar to a Fabry-Perot cavity, which has an input and output mirror with a field reflectivity $(1 - \kappa)$ and a fully reflecting mirror. κ is the coupling coefficient, $x = \exp(-\alpha L/2)$ represents a roundtrip loss coefficient, $\phi_0 = kLn_0$ and $\phi_{NL} = kLn_2|E_{in}|^2$ are the linear and nonlinear phase shifts, $k = 2\pi/\lambda$ is the wave propagation number in a vacuum, and L and α are the waveguide length and linear absorption coefficient, respectively. In this work, the iterative method is introduced to obtain the results as shown in Eq. (3), similarly, when the output field is connected and input into the other ring resonators.

An experimental setup of the multisoliton generation is shown in Figure 1. The system consists of an erbium-doped fiber amplifier (EDFA), a semiconductor optical amplifier (SOA), a fiber ring resonator, and a 90:10 output coupler. The EDFA was constructed using a 5 m length of EDF with erbium concentration of 950 ppm. The EDF is pumped by a 980 nm laser diode (LD) at a pumped power of 66.0 mW. Wavelength division multiplexer is used to combine the pump and laser wavelength. An SOA is incorporated in the ring cavity to amplify the signal from the EDFA. A ring resonator was constructed using a 3 dB coupler. A polarization controller (PC) and 3 m length of polarization-maintaining fiber (PMF) are included within the system. The principle of ring resonator is related to interferometer in which the four port optical coupler with two inputs and two outputs with 50:50 splitting ratio. The light beam is split into two beams, in which one propagates round the fiber ring, whereas the other propagates through the straight fiber. One of the beam polarization states is adjusted by

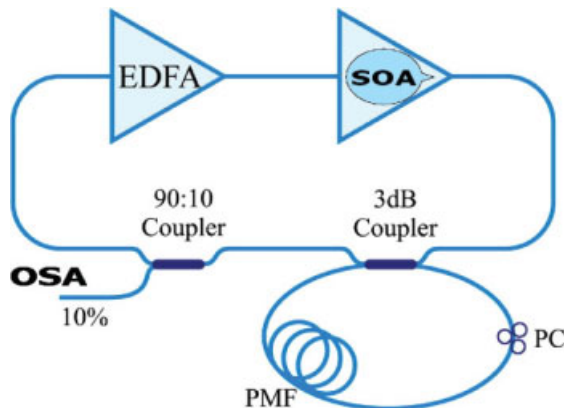


Figure 1 The experimental setup. EDFA, erbium-doped fiber amplifier; SOA, semiconductor optical amplifier; PC, polarization controller; PMF, polarization-maintaining fiber. [Color figure can be viewed in the online issue, which is available at www.interscience.wiley.com]

using a PC within the fiber ring, and this produces a slicing effect, whereas the intensity is dependent on the interference of the two beams at the PMF. The change in fiber birefringence effects the change in fiber refractive index. The multisoliton band can be generated by adjusting the fiber ring radius and the birefringence, whereas the modulation signals, that is, multisoliton pulses can be observed. A 90:10 output coupler is used to tap the output of the ring cavity laser. The output signal is characterized using an ANRITSU optical spectrum analyzer (OSA) with resolution of 50 pm.

In the first experiment with a standard EDFA configuration, the amplified spontaneous emission (ASE) occurs concurrently with signal amplification. This consequently causes the increase of noise configuration. As the LD was pumped by using a forward pumping scheme, a better noise figure was obtained. Figure 2 shows the ASE spectral taking after being slice by a ring resonator. As depicted in this figure, the ASE power obtained around 1530 nm, where more spontaneous emission occurs at that region. The maximum amplified power is at -49.19 dBm, the ASE spectrum then is looped back to the EDFA. The measurement is formed by using 10% of the output spectrum being coupled by the ring cavity by 90:10 output coupling and observed at OSA. Figure 3 shows the EDF lasing spectrum, whereas the bandwidth of the lasing spectrum is 14.3 nm with the maximum lasing power of 5.94 dBm.

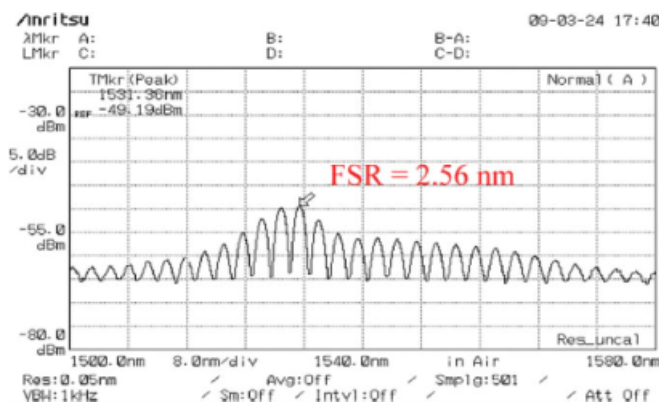


Figure 2 Result of the ASE of EDFA. [Color figure can be viewed in the online issue, which is available at www.interscience.wiley.com]

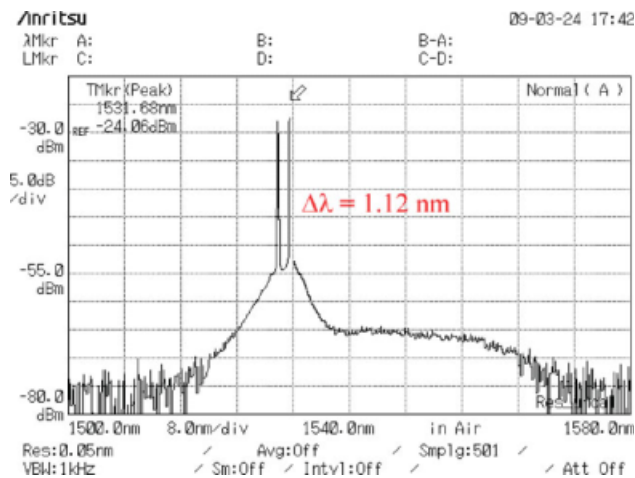


Figure 3 Result of the spectrum of EDF lasing spectrum. [Color figure can be viewed in the online issue, which is available at www.interscience.wiley.com]

In the second experiment, the multiwavelength, that is, multisoliton investigation for SOA with the saturated power (maximum bias current) of about 10 dBm (400 mA) is investigated. The operating temperature of the SOA is set at 30°C with the bias current of 200 mA. The ASE of SOA taken after the ring resonator is as shown in Figure 4. The extension ratio and the spacing between two peaks are dependent on the length of the PMF. In Figure 5, the multisoliton pulses are generated with the center wavelength at $1.54 \mu\text{m}$. The generation of multisoliton with a free spectrum range and spectrum width of 2.4 and 0.96 nm is achieved. The memory time of 15 min and the maximum output of -6.0 dBm are noted, respectively.

3. CONCLUSIONS

In conclusion, a generation of multiwavelength laser, that is, soliton is demonstrated, whereas the multisoliton pulses are also generated when the flat amplified output is seen. A ring resonator is used incorporating an SOA and EDFA in a ring cavity configuration to generate a comb filter for multiwavelength generation. The number of wavelength generated can be controlled

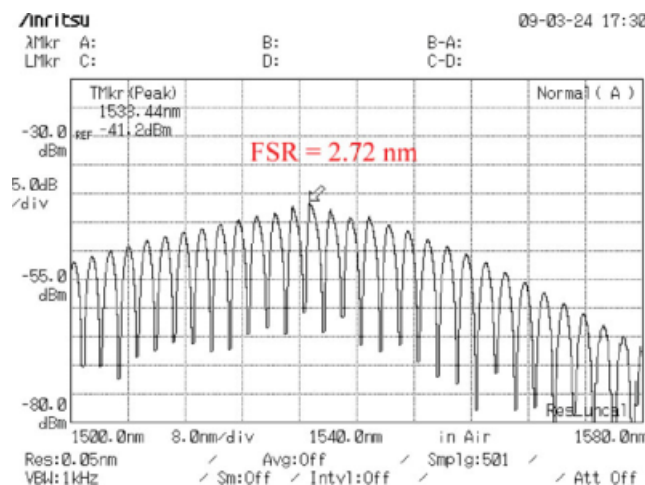


Figure 4 Result of a multiwavelength generation. [Color figure can be viewed in the online issue, which is available at www.interscience.wiley.com]

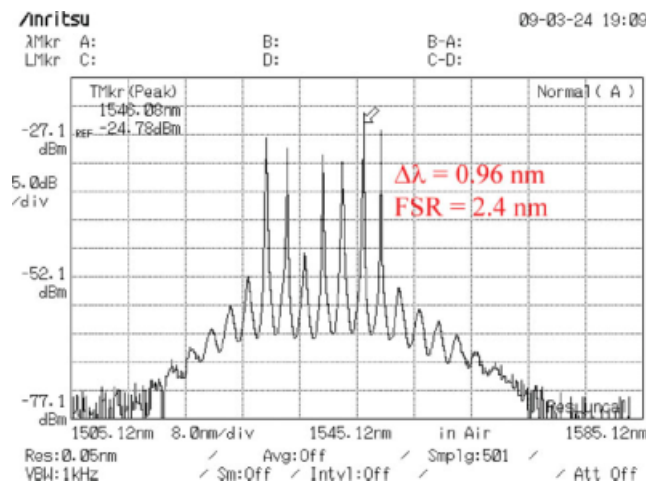


Figure 5 Result of a multisoliton band with center wavelength at $1.54 \mu\text{m}$. [Color figure can be viewed in the online issue, which is available at www.interscience.wiley.com]

by adjusting the SOA bias current, whereas the channel spacing and output spectrum bandwidth can be controlled by adjusting the birefringence in the ring cavity using the 3 dB couplers and the PCs. Results obtained have shown that more than 30 channels at a spacing of 2.4 nm and power of more than -0.6 dBm can be achieved, and the memory time of 15 min is noted.

REFERENCES

1. N. Pornsuwancharoen, U. Dunmeekaew, and P.P. Yupapin, Multi-soliton generation using a micro ring resonator system for DWDM based soliton communication, *Microwave Opt Technol Lett* 51 (2009), 1374–1377.
2. D. Deng and Q. Guo, Ince-Gaussian solitons in strongly nonlocal nonlinear media, *Opt Lett* 32 (2007), 3206–3208.
3. A. Hasegawa (Ed.), *Massive WDM and TDM Soliton transmission systems*, Kluwer Academic Publishers, Boston, 2000.
4. G.P. Agrawal, *Nonlinear fiber optics*, Academic Press, New York, 1995.
5. Yu.A. Simonov and J.A. Tjon, Soliton-soliton interaction in confining models, *Phys Lett B* 85 (1979), 380–384.
6. J.K. Drohm, L.P. Kok, Yu.A. Simonov, J.A. Tjon, and A.I. Veselov, Collision and rotation of solitons in three space-time dimensions, *Phys Lett B* 101 (1981), 204–208.
7. T. Iizuka and Y.S. Kivshar, Optical gap solitons in nonresonant quadratic media, *Phys Rev E* 59 (1999), 7148–7151.
8. R. Ganapathy, K. Porsezian, A. Hasegawa, and V.N. Serkin, Soliton interaction under soliton dispersion management, *IEEE Quantum Electron* 44 (2008), 383–390.
9. S.W. Harun, S. Shahi, A.H. Suraiman, and H. Ahmad, Multi-wavelength source based on SOA and EDFA in a ring cavity resonator, *Optoelectron Adv Mater* 2 (2008), 317–319.
10. P.P. Yupapin, P. Saeung, and C. Li, Characteristics of complementary ring-resonator add/drop filters modeling by using graphical approach, *Opt Commun* 272 (2007), 81–86.

© 2009 Wiley Periodicals, Inc.

INDUCTIVE MATCHING TECHNIQUE FOR A FEED-FORWARD NOISE-CANCELING CMOS LOW-NOISE AMPLIFIER

Hwann-Kaeo Chiou, Chin-Lung Li, Hsien-Yuan Liao, and Sung-Huang Lee

Department of Electrical Engineering, National Central University, No. 300, Jhongda Rd., Jhongli City, Taoyuan County 32001, Taiwan, Republic Of China; Corresponding author: hkchiou@ee.ncu.edu.tw

Received 2 April 2009

ABSTRACT: An inductive matching technique is proposed for a noise-canceling CMOS low-noise amplifier (LNA). This composite LNA consists of a main amplifier and a feed-forward amplifier. The feed-forward amplifier provides a noise canceling path to eliminate the noise at the output of the main amplifier. An inductor is used to tune out the remaining capacitive impedance at the output common node of two amplifiers, which provides the proper phase difference to cancel the overall noise voltage. For an optimum noise canceling bias, the measured noise figure is 2.5 dB, which is an improvement of 0.6 dB. © 2009 Wiley Periodicals, Inc. *Microwave Opt Technol Lett* 52: 72–75, 2010; Published online in Wiley InterScience (www.interscience.wiley.com). DOI 10.1002/mop.24838

Key words: inductive matching; noise-canceling; low-noise amplifier; feed-forward; composite LNA

1. INTRODUCTION

Recently, the radio frequency circuits implemented in CMOS technology are maturing. Low-noise amplifier (LNA) is the first amplification block in wireless receivers and plays an important role in overall performance of sensitivity, linearity, and power consumption of the receiver. The inductive source degeneration technique is widely used in an LNA design. However, the large inductor with low quality factor not only costs large area but also leads to high power dissipation. Many studies have been devoted to reduce the noise figure (NF) of LNA. Han et al. developed a complete thermal noise model of deep submicron MOSFETs considering the velocity saturation and carrier heating effects, which achieves an excellent NF at 5.2 GHz [1]. Chiu et al. thin down the substrate to $20 \mu\text{m}$ to suppress the substrate loss and obtain a NF of 2.17 dB at 5.2 GHz [2]. Asgaran et al. considered the gate resistance and proposed an LC network for input matching network, which yields a low power consumption of 4 mW [3]. However, in the techniques mentioned earlier, the best NF is achieved either by using accurate in-house noise model or extra postprocess such as substrate thinning. These techniques are not available in standard CMOS technology. Some LNAs are recently designed using standard process, for instance, Mou et al. suggested adopting a parallel LC network to replace the large gate inductor that therefore reduces the source inductance [4]. Lu et al. implemented a 2.4/5.2 GHz dual-band LNA by switching the input transconductance and the output capacitance to obtain a 3.7 dB NF at 5.2 GHz [5]. Bevilacqua et al. realized a wideband differential LNA in $0.13\text{-}\mu\text{m}$ CMOS process and obtain a NF of 3.5 dB [6]. These approaches using impedance match technique or differential topology still suffer from the trade-off between NF and input matching. The aforementioned techniques usually achieve NF around 3.5 dB at 5 GHz band. These results are about 1 dB worse than that using in-house noise model or extra postprocess. Brucoleri et al. developed a noise canceling technique by adopting a feed-forward amplifier in parallel to the main amplifier and the noise can be canceled by opposite phase at the output port [7–9]. This